

D5.4

NEMMO Ageing, Fouling and Wear Behavioural Modelling

Lead Beneficiary	DCU
Delivery date	2023-26-07
Dissemination level	Public
Status	Public
Version	1.0
Keywords	Multi-material, Wear, Ageing, Biofouling, Composite materials, Modelling



This project has received funding from the European Union's Horizon 2020 research and innovation programme under grant agreement No 815278.

www.nemmo.eu  [@NEMMO_Project](https://twitter.com/NEMMO_Project)  info@nemmo.eu

Information

Grant Agreement Number	815278
Project Acronym	NEMMO
Work Package	5
Task(s)	5.1
Deliverable	D5.4
Title	Deliverable 5.4 NEMMO Ageing, Fouling and Wear Behavioural Modelling
Author(s)	Adrián Delgado Ollero, Yan Delauré, Fiona Regan, Jean-Baptiste Jorcin,
File Name	NEMMO_D5.4_NEMMO_Ageing_Fouling_and_Wear_Behavioural_Modelling

Change Record

Revision	Date	Description	Reviewer
1.1	1 st June 2023	Initial Draft	Yan Delauré
1.2	16 th June 2023	Biofouling modelling	Adrián Delgado Ollero
1.3	29 th June 2023	Tecnalia contribution	Jean-Baptiste Jorcin
1.4	30 th June 2023	Review by Funditec	Dulce Muñoz
1.5	26 th July 2023	Final review	Pablo Benguria



1. Executive Summary

The NEMMO Research and Innovation Action project is funded by the European Commission under its Horizon 2020 framework programme. The project was approved under call LC-SC3-RES-11-2018: Building a Low-Carbon, Climate Resilient Future: Secure, Clean and Efficient Energy. This Deliverable 5.4 describes key findings from research carried out to develop new models for the ageing, biofouling and wear of tidal turbine materials. This work is now complete, and this report is intended to summarize key results. An outline of methodologies developed and implemented are presented first. Sample test results are then summarized covering the three components of material degradation which are ageing, wear and biofouling.

A series of accelerated ageing, and natural ageing at two locations were performed but showed limited impact on the composite material samples tested. Similarly, samples tested dynamically by exposure to cyclic hydrodynamic shear stresses over a six-month period did not show significant wear. The cyclic stress tests did however show a clear dependence between biofouling growth and hydrodynamics shear stress. A biofouling behavioural model inspired by elements of Avrami's model adapted to better suit micro and macro biofouling growth over several months of immersion has been proposed and tested. It relies on a sigmoid functional description to capture the typical growth-phases of biofouling. Results presented in this report cover three of the five material solutions tested as detailed in Deliverable D4.4 and confirm that the model can capture the full process from the initial latency phase to the exponential and then asymptotic phases. The functional parameters clearly show the dependence of biofouling growth to both material properties and hydrodynamics stresses.



Table of Contents

1.	Executive Summary	3
2.	Introduction	6
2.1	Objectives and outline	6
3.	Ageing	8
	References	9
4.	Biofouling	10
4.1	Why a biofouling growth model is needed	10
4.2	Avrami's model	11
4.3	Biofouling growth study using supervised image classification	11
4.4	Wear	15
5.	Conclusions	16
	References	16



INTRODUCTION



2. Introduction

2.1 Objectives and outline

This deliverable presents key research results from the study of material wear, ageing and biofouling. The primary aim of the research was to develop new behavioural model to help predict how turbine blade material will age, wear and biofouling when exposed to nominal operating conditions. New methodologies have been developed to provide data against which to calibrate the models. These along with relevant data have been presented in D4.4 (Report on Best Performing Biomimetic and multi-material solutions for tidal turbine composite blades) and D4.5 (Public report on NEMMO testing campaign for behavioural modelling of tidal turbine composite blades including large scale composite blade testing). The present report focuses instead on the models and their assessments. Several candidate materials have been tested and are considered in the report.

The report reviews the three model in turn and includes four sections:

- Section 1: Introduction. Main purpose and structure of the report.
- Section 2: Ageing model.
- Section 3: Biofouling and wear model.

The document is intended for all stakeholders and for public dissemination.



TASK 5.1 AGEING, FOULING AND WEAR BEHAVIOURAL MODELLING



3. Ageing

In a first phase of the NEMMO project (WP2), an assessment of the behaviour of the composite material initially used, a glass fibre reinforced vinyl ester, was done before and after ageing according to three different protocols:

- Accelerated ageing test in laboratory following the protocol defined during the WP2 activities
- Natural ageing of 6 months in immersion in the port of Pasaia (Gipuzkoa, Spain)
- Natural ageing of 6 months in immersion in the HarshLab, which is an offshore floating infrastructure moored in the Cantabrian Sea close to the locality of Armintza (Bizkaia, Spain)

Then, in a second phase, new materials were developed, considering enhanced composite material with the addition of carbon Nanotubes or additive to intend to improve mechanical properties and surface coating with the addition of nanoparticles to intend to improve the anti-fouling capabilities.

The following (part of the activities of the WP4) steps consisted in performing the ageing of these new material following the three protocols mentioned above.

The final step would consist in analysing the effect of the ageing on the materials studied to intend to define a degradation model that ideally would allow to calculate lifetime estimation. The ageing related to this section considers only the physicochemical ageing in static condition without mechanical load.

A literature review of polymer degradation(1–5) indicates that only few degradation mechanisms remains relevant for natural sea water degradation. Obviously, thermolysis (degradation above 60°C) can be eliminated. As it was shown in the D2.4, the UV ageing did not affect the material and thus photo-oxidation can also be eliminated. Finally, vinyl ester are quite stable polymer and the biodegradation kinetic is quite slow. It remains only water uptake and swelling as possible option for degradation mechanism. The water uptake would induce a plasticization of the polymeric matrix, leading to a loose of mechanical properties and it would also weaken the link between the fibres and the matrix, affecting the shear properties of the material.

The paper of Krauklis *et al.* (6) present a quite complete and extensive polymer degradation model, taking account of the water penetration and diffusion in the composite among other parameters to simulate the water uptake and to estimate the effect on the mechanical properties.

Nevertheless, due to the small resources attributed to Tecnia (1 person-month for the full WP5) for this activity, the adaptation of this model to the NEMMO materials couldn't be achieve. In addition, it appears after the WP4 results analysis that the data gathers were not adequate to feed and calibrate such model. The gravimetric measurements that were initially aiming to assess the composite water uptake were totally bias due to the formation of fouling. The only relevant gravimetric measurements were for the accelerated ageing test, that appear to be not enough long (even if it took a large time in the project timeline) to be relevant. The same dynamic happened with the tensile tests.

In a general matter, all the material tested appeared to be very stable in immersion in sea water during the testing time allowed by the project. On the positive side, it is good news as the initial material selection was good and the materials are suitable for such environment. On the negative side, the lack of measurable degradation effect does not allow to define a degradation model.



References

1. Davies P, Rajapakse YDS, editors. *Durability of Composites in a Marine Environment* [Internet]. Springer Netherlands; 2014 [cited 2021 Jun 2]. (Solid Mechanics and Its Applications). Available from: <https://www.springer.com/gp/book/9789400774162>
2. Davies P. Environmental degradation of composites for marine structures: new materials and new applications. *Philos Transact A Math Phys Eng Sci* [Internet]. 2016 Jul 13 [cited 2021 Jun 3];374(2071). Available from: <https://www.ncbi.nlm.nih.gov/pmc/articles/PMC4901245/>
3. Singh B, Sharma N. Mechanistic implications of plastic degradation. *Polym Degrad Stab*. 2008 Mar 1;93(3):561–84.
4. Rånby B. Photodegradation and photo-oxidation of synthetic polymers. *J Anal Appl Pyrolysis*. 1989 Mar 1;15:237–47.
5. Boisseau A, Davies P, Thiebaud F. Sea Water Ageing of Composites for Ocean Energy Conversion Systems: Influence of Glass Fibre Type on Static Behaviour. *Appl Compos Mater*. 2012 Jun 1;19(3):459–73.
6. Krauklis AE, Karl CW, Rocha IBCM, Burlakovs J, Ozola-Davidane R, Gagani AI, et al. Modelling of Environmental Ageing of Polymers and Polymer Composites—Modular and Multiscale Methods. *Polymers*. 2022 Jan 5;14(1):216.



4. Biofouling

4.1 Why a biofouling growth model is needed

Only a few studies have attempted to provide models aimed at describing and predicting the growth of biofouling on different materials. For example, marine structures, once built are inevitably subject to colonization by micro-organisms that can induce aesthetic but also mechanical degradation. These micro-organisms can be bacteria, algae, fungi, lichens and others. It has been proven that, except for ubiquitous bacteria, algae are the first colonizers. The establishment of micro-organisms depends on various parameters of origin. In temperate or tropical climates, the composition of a biofilm and the dominant species can be substantially different [1]. According to several authors, in an ecosystem, the microclimate to which samples are subjected is regulated by different parameters that control the nature and growth of microorganisms [2,3]. The microclimate is influenced by sun exposure, water flow velocity, nutrients in the water, depth and temperature. Substrate characteristics, such as porosity, surface roughness, chemical composition and surface pH, are obviously important [4–6]. Several studies have focused on the influence of these parameters on biofouling, both at laboratory and full-scale. However, to our knowledge, very few studies have attempted to model this phenomenon. Studies conducted by B. Chen-Charpentier and co-workers developed a numerical simulation of biofilm growth in porous materials [7]. The biofouling of algae growing on porous materials was calculated by mathematical modelling using a system of hyperbolic-elliptic partial differential equations. Thanks to this mathematical modelling, it was found that the physical phenomenon of algal cell growth and multiplication generally follows a trend similar to a sigmoidal curve [8]. In fact, microalgae culture growth is characterized by three phases; an initial lag phase in which the algae begin to adapt to the growing conditions called "latency time", a phase of rapid exponential growth and finally a stationary phase, in which the surface area covered remains constant over time (Figure 1).

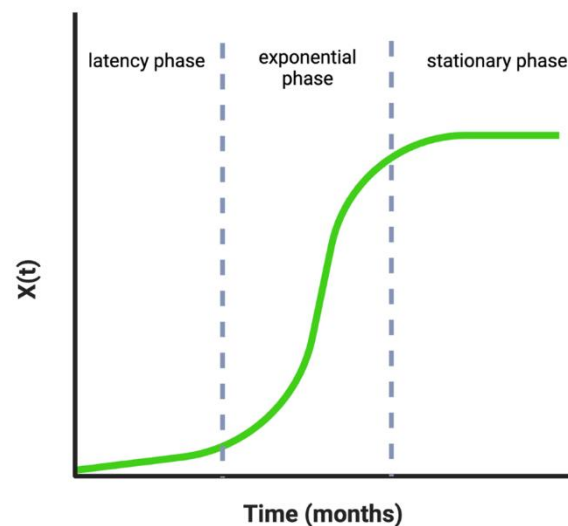


Figure 1: Typical growth-phases of an algae culture



4.2 Avrami's model

Additional studies by Ruot and Barberousse showed that it was possible to study the process of biofouling under accelerated conditions under highly regulated conditions in the laboratory using Avrami's law applied to specific points for a single organism [9]. Avrami's law was developed in the form of an exponential equation by Avrami, Johnson and Melh [10–13]. This law was originally used to describe the kinetic phase transformation of solids [14,15], although it is used in different fields: crystallisation of polymers, heat treatment or solids decomposition [16,17]. For example, it is a model commonly used to study the formation of ice crops in the different layers of the atmosphere. This mathematical model mainly has two phases, nucleation, which corresponds to the appearance of a nucleus that gives rise to a new phase and on which the second phase takes place, which is the expansion or growth phase in which this nucleus begins to grow larger over time (Figure 2). In the same way, the process of biofouling in different materials can be described by means of these two phases.

In the colonisation phase, organisms begin by attaching to the substrate. Specifically, the primary colonisers, in this case microscopic algae such as diatoms and/or benthic cyanobacteria, adhere to the surface, identified as green spots that correspond to the nucleation points of Avrami's model. From then on, this nucleation point will expand over time, which corresponds to the growth phase.

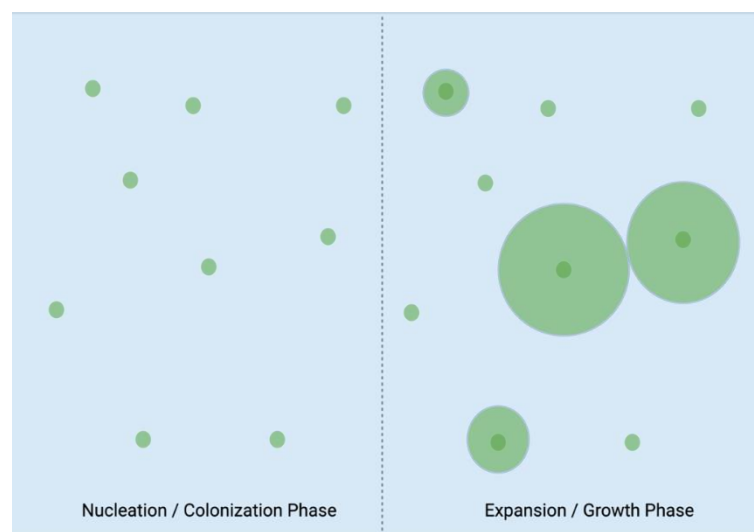


Figure 2: Simplified representation of Avrami's model. Transformation of one phase from another by the growth of randomly formed nuclei. Each dot represents a colonizing organism like a microscopic alga (image on the right) that is expanding/growing (image on the left).

4.3 Biofouling growth study using supervised image classification

In this biofouling study, the possibility of using this method for the calculation of biofouling growth was considered. However, one of the negative points of this Avrami's model is that it can only be applied to a certain group of organisms (microscopic algae) for a short period of time (1-2 weeks). It cannot be adapted for a prolonged deployment of several months at sea to assess the growth of



macroscopic species such as barnacles or tunicates. In addition, in Avrami's model, the chromatic change is used for the calculation of the covered surfaces. In our experiments the changes in colour and luminosity are not constant because they are field studies and the submerged samples are exposed to chemical oxidation and above all to numerous organisms of different colour, shape and size. This is why we discarded the possibility of using Avrami's model and proceeded to create a sigmoidal model to explain the growth in a similar way, but using techniques based on image classification by artificial vision techniques using machine learning algorithms in a fast way that could be applied to a wide range of materials and biofouling studies.

Currently, biofouling quantification is often a painstaking, manual and complex task [18]. Increasingly stringent requirements of biofouling management are stimulating efforts to develop reliable methods to quantify, analyse and assess biofouling damage in a more efficient and rapid manner that allows different industries and sectors to evaluate which materials are better in terms of biofouling performance. To this end, the NEMMO project aimed to develop a rapid method to quantify, classify and evaluate the performance of different materials in marine renewable energy applications where surfaces are exposed to hydrodynamics shear stresses. In this case biofouling tends to be primarily from microscopic biofilms and in regions of lower shear stresses a mixture of biofilms and hard shell macro fouling. The method to acquire the visual data used to develop these biofouling behavioural models is detailed in the NEMMO deliverable D4.4.

To construct a regression model for biofouling growth, we utilized the segmentation maps generated through TWS (Time-Weighted Sedimentation) in conjunction with a plugin provided by the Swiss Federal Institute of Technology Lausanne. This plugin facilitated the determination of the total percentage of surface area covered by each colour within the segmentation map or vector. The areas covered by the three biofouling classes (slime, hard, and soft) were aggregated for each triplicate, and the mean value was calculated. Subsequently, the average values representing the percentage of total biofouling coverage for each material were plotted for each month.

To fit the graphical representations, a 4-parameter sigmoidal regression (Eq. 1) was applied using Sigmaplot version 11 (build 11.0.0.77) by Systat Software, Inc, based in California, United States. The default number of interactions was set to 200 in order to achieve the optimal fit. A tolerance level of 1×10^{-10} was utilized, and parameter standard errors in weighted regression were computed using the Chi-Square method. The normality of the data was assessed through the Shapiro-Wilk test, with a sample size limit of ≤ 5000 and a rejection threshold (P-Value) of 0.05. Subsequently, we focused on studying the exponential growth phase from the key function parameters.

$$Y = Y_0 + \left(\frac{a}{1 + e^{-\left(\frac{x-x_0}{b}\right)}} \right) \quad (\text{Eq 1})$$

There are four such function parameters: Y_0 , x_0 , a and $1/b$. The initial biofouling coverage is represented by Y_0 . This should be negligible for a clean surface at immersion and is not critical in this study. The delay due to the latency phase and the initial part of the exponential phase is captured by x_0 . The biofouling coverage at the end of the stationary phase is measured by a while the rate of relaxation that is the slowdown in the growth of biofouling coverage at the end of the exponential phase is given by $1/b$. The three parameters a , x_0 and $1/b$ have been used to compare the growth and colonization rates between the various materials tested.



The NEMMO deliverable D4.4 provide a detailed description of the dynamic test campaign used to characterise the antifouling performance of five candidate material solutions under characteristic hydrodynamic conditions. This data has been used to test the suitability of the proposed sigmoid representation of biofouling growth taking account of material properties and surface hydrodynamic stresses. Results from three sample materials are presented here. These include a solvent based polyurethane resin with silica nano-particles (C15 SiO₂), a control composite made with the coating used on the original Magallanes hydro-turbine blade (Control) and a water based polyurethane resin (PUD). The data was acquired at three radial positions on the test turbine (*P1*, *P2* and *P3*) where hydrodynamic surface stresses were estimated to be approximately 60 Pa, 230 Pa and 270 Pa respectively and results are shown in Figure 3, Figure 4 and Figure 5.

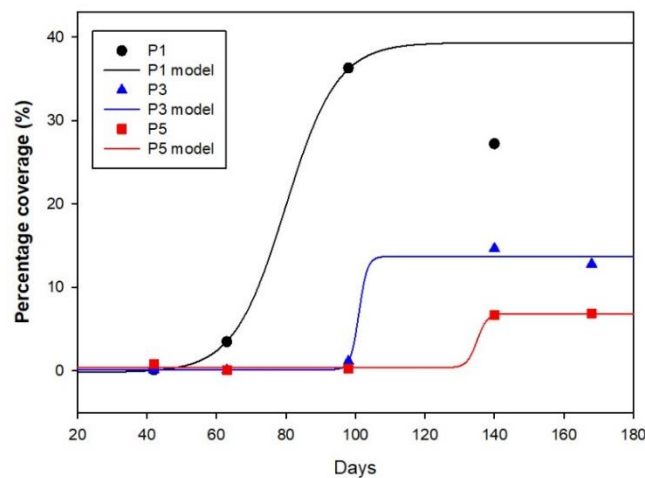


Figure 3 Evolution of biofouling coverage for C15 SiO₂ coating from 24 week test campaign and measurements at location *P1*, *P2* and *P3*. The continuous lines represent the fitted sigmoid curves.

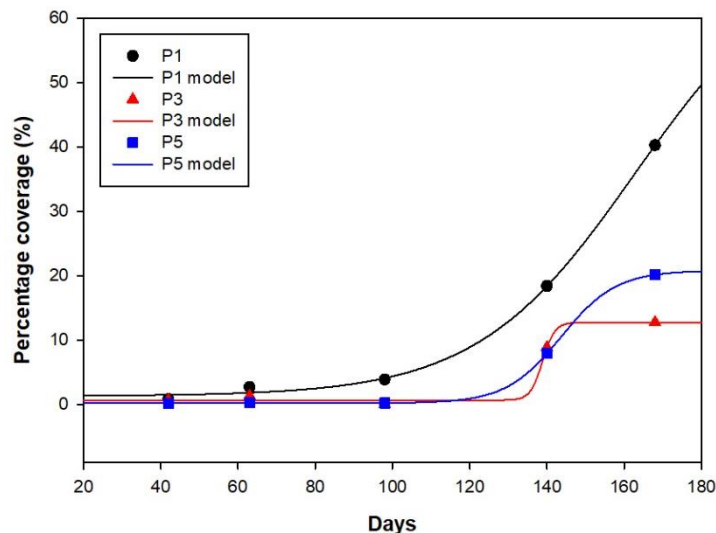


Figure 4 Evolution of biofouling coverage for Control coating from 24 week test campaign and measurements at location *P1*, *P2* and *P3*. The continuous lines represent the fitted sigmoid curves.



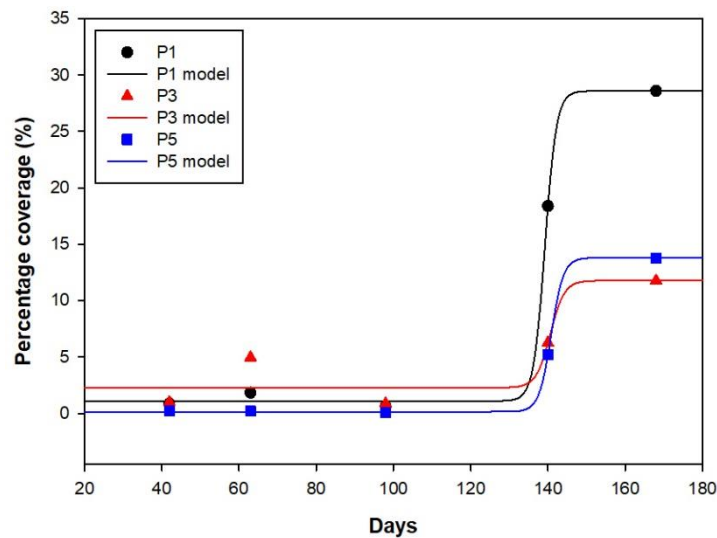


Figure 5. Evolution of biofouling coverage for PUD coating from 24 week test campaign and measurements at location *P1*, *P2* and *P3*. The continuous lines represent the fitted sigmoid curves.

The model parameters are compared in Table 1 and clearly show that the increases in surface stresses between *P1* and *P3* consistently reduces the asymptotic cover for all materials. Beyond *P3* to *P5* the change is not as consistent. While the asymptotic cover decreases with C15 SiO₂ the opposite is observed with PUD and the control coating. In all cases however the change is small and biofouling at both *P3* and *P5* is exclusively from biofilm rather than the mix of biofilm and hard shell macro fouling seen at *P1*. From the data shown here, the C15 SiO₂ outperforms other coating where surface stresses are higher. It is also interesting to note that the material is also shown to have the capacity to generally delay the exponential growth phase.

Table 1. Sigmoid parameters for different sample coatings and hydrodynamic stresses

		Y_0 Initial cover	a Asymptotic cover	x_0 Latency delay	b Rate of relaxation
C15 SiO ₂	<i>P1</i>	0	39.5	80	0.13
	<i>P3</i>	0	13.6	101	0.8
	<i>P5</i>	0.4	6.5	135	0.7
Control	<i>P1</i>	1.3	69.1	163	0.05
	<i>P3</i>	0.7	12.1	139	0.6
	<i>P5</i>	0.2	20.6	144	0.14
PUD	<i>P1</i>	1.1	27.5	139	0.6
	<i>P3</i>	2.3	9.5	140	0.5
	<i>P5</i>	0.1	13.6	140	0.6



4.4 Wear

The wear analysis was performed to assess the effect of combined exposure to the marine environment and hydrodynamic stresses. The types of wear possible include delamination, scoring or fatigue fracturing. These can be easily identified from surface imaging without needing laboratory based analysis. More benign effects including micro scoring can affect hydrodynamic performance of a turbine blade due to increase in surface roughness. Its analysis however would require disruptive dismantling and testing which would have interfered with the primary aim of the study which focussed on biofouling assessment. To avoid this, samples were not removed from the turbine for the full duration of the tests and were imaged regularly to evaluate the biofouling growth. Results indicate that none of the samples including the biomimetic textures investigated in NEMMO experienced significant wear or degradation except for the PUD coating. This coating experienced significant delamination after 15 weeks of immersion and periodic daily hydrodynamic shearing. The biofouling including barnacles that have grown over the first 15 weeks of immersion can be seen on Figure 6 to reduce significantly between weeks 15 and 21 as a result of this surface damage.

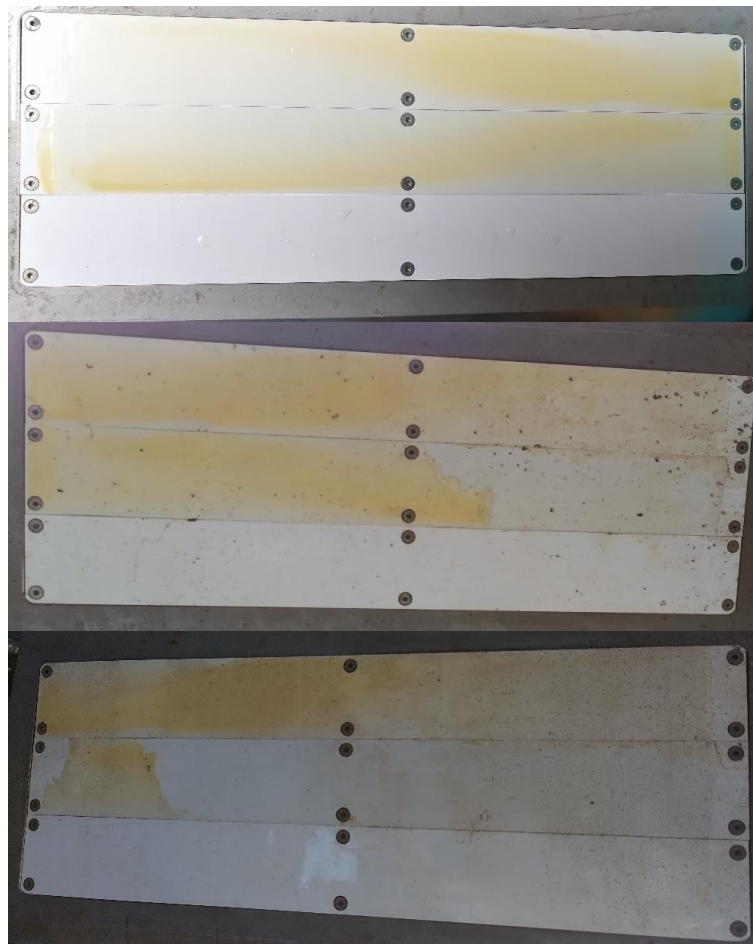


Figure 6 Images of the PUD coated samples (middle and top plates on the impeller), [Top] Image taken after 2 weeks of immersion, [Middle] Image taken after 15 weeks of immersion, [Bottom] Image taken after 21 weeks immersion.



5. Conclusions

Biofouling data from a 24-week marine test campaign conducted between December 2022 and June 2023 has been used to test the feasibility of modelling biofouling growth. Samples tested were immersed on the four flat surfaces of a vertical axis two blade impeller and exposed to periodic hydrodynamic shear stress cycles. The test campaign was designed to emulate conditions over a hydroturbine surfaces but relied on daily cycles of 30-minute impeller rotation chosen to accelerate biofouling settlement by allowing early stage settling organisms several hours every day to form a more secure initial attachment. Five candidate samples developed and built for the NEMMO project for their expected antifouling properties were included in the study. Results presented in this public deliverable cover three of these material coatings including the best performing solution based on a solvent based polyurethane coating which incorporates SiO₂ nanoparticles. The full set of results is detailed in the confidential deliverable D4.4. The new behavioural biofouling model proposed relies on a sigmoid function to capture the three phases of growth which are the latency, exponential and stationary phases. The data presented here confirms its suitability. Key functional parameters are shown to provide an effective way to quantify growth and allows for an easier comparison of impact of materials on biofouling.

References

1. Crispim, C.A.; Gaylarde, P.M.; Gaylarde, C.C. Algal and Cyanobacterial Biofilms on Calcareous Historic Buildings. *Curr Microbiol* **2003**, *46*, 79–82, doi:10.1007/S00284-002-3815-5.
2. Ariño, X.; Gomez-Bolea, A.; Saiz-Jimenez, C. Lichens on Ancient Mortars. *Int Biodeterior Biodegradation* **1997**, *40*, 217–224, doi:10.1016/S0964-8305(97)00036-X.
3. John; D.M Algal Growth on Buildings: A General Review and Methods of Treatment. *Int Biodeterior Biodegradation* **1988**, *2*, 81–102.
4. Ortega-Calvo, J.J.; Ariño, X.; Hernandez-Marine, M.; Saiz-Jimenez, C. Factors Affecting the Weathering and Colonization of Monuments by Phototrophic Microorganisms. *Science of The Total Environment* **1995**, *167*, 329–341, doi:10.1016/0048-9697(95)04593-P.
5. Tomaselli, L.; Lamenti, G.; Bosco, M.; Tiano, P. Biodiversity of Photosynthetic Micro-Organisms Dwelling on Stone Monuments. *Int Biodeterior Biodegradation* **2000**, *46*, 251–258, doi:10.1016/S0964-8305(00)00078-0.
6. Tran, T.H.; Govin, A.; Guyonnet, R.; Grosseau, P.; Lors, C.; Garcia-Diaz, E.; Damidot, D.; Devès, O.; Ruot, B. Influence of the Intrinsic Characteristics of Mortars on Biofouling by Klebsormidium Flaccidum. *Int Biodeterior Biodegradation* **2012**, *70*, 31–39, doi:10.1016/J.IBIOD.2011.10.017.
7. Chen-Charpentier, B. Numerical Simulation of Biofilm Growth in Porous Media. *J Comput Appl Math* **1999**, *103*, 55–66, doi:10.1016/S0377-0427(98)00240-4.
8. Tran, T.H.; Govin, A.; Guyonnet, R.; Grosseau, P.; Lors, C.; Damidot, D.; Devès, O.; Ruot, B. Avrami's Law Based Kinetic Modeling of Colonization of Mortar Surface by Alga Klebsormidium Flaccidum. *Int Biodeterior Biodegradation* **2013**, *79*, 73–80, doi:10.1016/j.ibiod.2012.12.012.



9. Barberousse, H.; Ruot, B.; Yéprémian, C.; Boulon, G. An Assessment of Façade Coatings against Colonisation by Aerial Algae and Cyanobacteria. *Build Environ* **2007**, *42*, 2555–2561, doi:10.1016/J.BUILDENV.2006.07.031.
10. Avrami, M. Kinetics of Phase Change. I General Theory. *J Chem Phys* **2004**, *7*, 1103, doi:10.1063/1.1750380.
11. Avrami, M. Kinetics of Phase Change. II Transformation-Time Relations for Random Distribution of Nuclei. *J Chem Phys* **2004**, *8*, 212, doi:10.1063/1.1750631.
12. Avrami, M. Granulation, Phase Change, and Microstructure Kinetics of Phase Change. III. *J Chem Phys* **2004**, *9*, 177, doi:10.1063/1.1750872.
13. William A. Johnson; Robert F. Mehl Reaction Kinetics in Processes of Nucleation and Growth. *American Institute of Mining and Metallurgical Engineers. Technical Publication* **1939**, *135*, 416.
14. Khawam, A.; Flanagan, D.R. Solid-State Kinetic Models: Basics and Mathematical Fundamentals. *J Phys Chem B* **2006**, *110*, 17315–17328, doi:10.1021/jp062746a.
15. Fanfoni, M.; Tomellini, M. The Johnson-Mehl- Avrami-Kohnogorov Model: A Brief Review. *Il Nuovo Cimento D 1998 20:7* **1998**, *20*, 1171–1182, doi:10.1007/BF03185527.
16. Slováček, M. Application of Numerical Simulation of Heat Treatment in Industry. *Journal de Physique IV* **2004**, *120*, 753–760, doi:10.1051/jp4:2004120087.
17. Hay, J.N. Application of the Modified Avrami Equations to Polymer Crystallisation Kinetics. *British Polymer Journal* **1971**, *3*, 74–82, doi:10.1002/pi.4980030205.
18. Butler, A.J.; Canning-Clode, J.; Coutts, A.D.M.; Cowie, P.R.; Dobretsov, S.; Dürr, S.; Faimali, M.; Lewis, J.A.; Page, H.M.; Pratten, J.; et al. Techniques for the Quantification of Biofouling. *Biofouling* **2010**, 319–332, doi:10.1002/9781444315462.CH22.

